Published in final edited form as:
*Radiat Res*. 2013 October ; 180(4): 367–375. doi:10.1667/RR3111.1.

# Gap Junction Communication and the Propagation of Bystander Effects Induced by Microbeam Irradiation in Human Fibroblast Cultures: The Impact of Radiation Quality

**Narongchai Autsavapromporn**[a], **Masao Suzuki**[a,1], **Tomoo Funayama**[b], **Noriko Usami**[c], **Ianik Plante**[d], **Yuichiro Yokota**[b], **Yasuko Mutou**[b], **Hiroko Ikeda**[b], **Katsumi Kobayashi**[c], **Yasuhiko Kobayashi**[b], **Yukio Uchihori**[e], **Tom K. Hei**[f], **Edouard I. Azzam**[g], and **Takeshi Murakami**[a]

[a]Research Center for Charged Particle Therapy, National Institute of Radiological Sciences, Chiba, 263-8555, Japan

[b]Microbeam Radiation Biology Group, Medical and Biotechnological Application Division, Quantum Beam Sciences Directorate, Japan Atomic Energy Agency, Takasaki, 370-1292, Japan

[c]Photon Factory, High Energy Accelerator Research Organization, Tsukuba, 305-0801, Japan

[d]University Space Research Association, NASA Johnson Space Center, Houston, Texas 77058

[e]Research, Development and Support Center, National Institute of Radiological Sciences, Chiba, 263-8555, Japan

[f]Center of Radiological Research, Columbia University Medical Center, New York, New York 10032

[g]Department of Radiology, Rutgers University, New Jersey Medical School, Cancer Center, Newark, New Jersey 07103

## Abstract

Understanding the mechanisms underlying the bystander effects of low doses/low fluences of low- or high-linear energy transfer (LET) radiation is relevant to radiotherapy and radiation protection. Here, we investigated the role of gap-junction intercellular communication (GJIC) in the propagation of stressful effects in confluent normal human fibroblast cultures wherein only 0.036–0.144% of cells in the population were traversed by primary radiation tracks. Confluent cells were exposed to graded doses from monochromatic 5.35 keV X ray (LET ~6 keV/μm), 18.3 MeV/u carbon ion (LET ~103 keV/μm), 13 MeV/u neon ion (LET ~380 keV/μm) or 11.5 MeV/u argon ion (LET ~1,260 keV/μm) microbeams in the presence or absence of 18-α-glycyrrhetinic acid (AGA), an inhibitor of GJIC. After 4 h incubation at 37°C, the cells were subcultured and assayed for micronucleus (MN) formation. Micronuclei were induced in a greater fraction of cells than expected based on the fraction of cells targeted by primary radiation, and the effect occurred in a dose-dependent manner with any of the radiation sources. Interestingly, MN formation for the heavy-ion microbeam irradiation in the absence of AGA was higher than in its presence at high



[1]Address for correspondence: Research Center for Charged Particle Therapy, National Institute of Radiological Sciences, Chiba, 263-8555, Japan; m_suzuki@nirs.go.jp.

mean absorbed doses. In contrast, there were no significant differences in cell cultures exposed to X-ray microbeam irradiation in presence or absence of AGA. This showed that the inhibition of GJIC depressed the enhancement of MN formation in bystander cells from cultures exposed to high-LET radiation but not low-LET radiation. Bystander cells recipient of growth medium harvested from 5.35 keV X-irradiated cultures experienced stress manifested in the form of excess micronucleus formation. Together, the results support the involvement of both junctional communication and secreted factor(s) in the propagation of radiation-induced stress to bystander cells. They highlight the important role of radiation quality and dose in the observed effects.

## INTRODUCTION

Recently, the traditional dogma that the important biological effects of radiation arise from changes induced solely in directly irradiated cells (targeted effect) has been challenged by the observation that similar effects can also be seen in nonirradiated cells, a phenomenon known as the bystander effect (1–6). Bystander studies have been carried out using microbeam and broad-beam irradiators capable of delivering low- or high-linear energy transfer (LET) radiation, co-culture approaches and the method of transferring growth medium from irradiated cells to bystander cells (1–16). Specifically, microbeams have the ability to deliver doses of ionizing radiation (IR) to selected individual cells or subcellular targets (6, 7, 10, 11, 14–16).

Radiation-induced bystander effects were clearly identified in 1992 by Nagasawa and Little when they observed that 20–40% of the cells in cultures wherein only 0.1–1% were traversed by an α-particle track exhibited excess sister chromatid exchanges (1). These results indicated that the cross section for inducing chromosomal damage by α particles was much larger than the nucleus or the cell itself. These findings were subsequently confirmed with a variety of biological endpoints such as cell killing, micronucleus (MN) formation, mutation, cell cycle arrest, oncogenic transformation, and changes in the levels of mRNA and proteins (2–17). The bystander effect has been observed in different types of cells exposed to various radiations. Both high- and low-LET radiation have been shown to induce a bystander response (1–17). However, the observations were not universal. In experiments involving human fibroblasts and transfer of growth medium, there was a lack of bystander effect being detected after low-LET irradiation but a significant effect being observed after high-LET irradiation (18). However, it is still unclear whether the bystander effect is likely related to radiation quality, cell type and/or the biological endpoints studied.

Several processes have been examined to elucidate the mechanisms underlying radiation-induced bystander effects. Gap-junction intercellular communications (GJIC), secreted diffusible factors released from irradiated cells, oxidative metabolism have all been advocated as mediators of bystander responses (1–7, 12–25). Among the different processes, direct evidence was generated for participation of GJIC (21). Junctional communication mediates propagation of stressful effects among irradiated cells and between irradiated cells and bystander cells (19–25). However, it remains undefined whether the GJIC-mediated propagation of a stressful effect in bystander cells is dependent on radiation quality (i.e., LET).

Gap junctions are dynamic structures that are critical for diverse physiological functions (26). The intercellular channels that comprise gap junctions are formed by connexins. Each of the 20 isoforms of connexin forms channels with distinct permeability properties. By allowing direct intercellular transfer of cytoplasmic molecules, they provide a powerful pathway for direct molecular signaling between neighboring cells. Although the properties of channels formed by each isoform differ, connexin pores are generally considered to allow permeation of molecules up to 1,000 Da, well above the size of most second messengers (26). In the current study, we investigated the effect of cell–cell communication by gap junctions on the induction of DNA damage in confluent human fibroblast cultures using various types of microbeams delivering radiation with LET ranging from ~6 to 1,260 keV/μm.

## MATERIALS AND METHODS

### Cell Culture

Early passage (passage 6–10) normal human skin fibroblasts (NB1RGB: cell no. RCB0222) were obtained from the RIKEN BioResource in Japan. The cells were cultured in Eagle's minimum essential medium (MEM: NISSUI Pharmaceutical, Japan) containing 10% fetal bovine serum (FBS: Hyclone, ThemoFisher Scientific) in a humidified atmosphere of 95% air/5% $CO_2$ at 37°C.

### X-Ray Microbeam Irradiation

Monochromatic X-ray microbeam irradiation was performed using the synchrotron X-ray microbeam irradiation apparatus installed at the BL-27B station in the Photon Factory, High Energy Accelerator Research Organization (KEK) in Tsukuba, Japan. The beam characteristics, biological irradiation procedures and dosimetry have been described (27, 28). Using this system, the cells were seeded, 2 days prior to irradiation, at a density of ~5 × $10^6$ cells/dish into specially designed microbeam dishes consisting of an acrylic resin ring of 36 mm in diameter and a 7.5 μm thick polyimide film on the bottom (Fig. 1A). At the time of irradiation, the cells were confluent, therefore allowing direct communication through gap junctions. About 95% of the cells were in the $G_1/G_0$ phase as analyzed by flow cytometry (data not shown), which eliminates complications in interpreting the results due to different effects being induced in cells at different phases of the cells cycle (29). Irradiation was carried out using the 256 (16 × 16) cross-strip method with a beam area of 20 × 20 μm (Fig. 1B). In our experiments, we re-used the acrylic resin ring and base after thorough washing and sterilization; only the polyimide film is disposable.

In this study, we did not specifically target the cell nucleus or cytoplasm because it has been reported that both nuclear and cytoplasmic irradiation are able to generate bystander responses (4–7). Sample microbeam dishes (containing MEM growth medium) were placed horizontal on the irradiation stage and the position of the irradiated area in the center of the microbeam dishes was determined automatically using a computer-controlled irradiation stage and a cooled charged coupled (CCD) camera (27). The exposure rate was measured with a specially designed free-air ionization chamber (28). When irradiated with a beam size of 20 × 20 μm as shown in Fig. 1, around 0.036–0.144% of the total cells attached on the

bottom of the microbeam dishes are hit by radiation. The irradiations were performed at room temperature under ambient conditions and the exposure time varied from 5 to 25 min depending on the dose. Control samples were handled in parallel but were sham irradiated.

In experiments conducted with 20 × 20-μm X-ray microbeams, the X-ray energy was mostly absorbed by the targeted area within the cell nucleus and/or cytoplasm. Under these conditions, the absorbed dose D (in Gy) for NB1RGB cells (Table 1) was calculated from the exposure, X (in C/kg) according to the following equation;

$$D = X \times W/e \times (\mu_{en}/\rho)_{NB1RGB}/(\mu_{en}/\rho)_{air}$$

Where $\mu_{en}/\rho$ is the mass energy deposition coefficient ($m^2/kg$); W, the energy required to generate an ion pair and *e*, the elementary electric charge. We considered the value of $\mu_{en}/\rho$ in soft tissue for NB1RGB cells (28). The energy of the X ray was 5.35 keV and the exposure rate was ~$7.7 \times 10^{-3}$ C $kg^{-1}$ $s^{-1}$ ($9.3 \times 10^3$ photon $s^{-1}$ 100 $\mu m^{-2}$), as measured with an AXUV-100 absolute XUV silicon photodiode (International Radiation Detectors Inc., Torrance, CA).

## Heavy-Ion Microbeam Irradiation

The heavy-ion microbeam facility of Takasaki Ion Accelerators for Advanced Radiation Application (TIARA) at Japan Atomic Energy Agency (JAEA) was used to deliver precise numbers of 18.3 MeV/u carbon ions, 13 MeV/u neon ions or 11.5 MeV/u argon ions with corresponding LET values in liquid water of ~103 keV/μm, ~380 keV/μm and ~1,260 keV/μm, respectively. The beam characteristics and dosimetry of heavy-ion microbeam irradiations have been described previously (22, 30). Briefly, particles traversing the film of the dish were detected by plastic scintillator and photomultiplier tube installed in an inverted microscope below the vertical beam line. The energy spectra of the detected ions were measured with a multichannel analyzer by analyzing the pulse height of the scintillation signals. The number of ions having traversed the sample was counted with a constant fraction discriminator coupled to a preset counter (22, 30).

The preparation of cell samples and the biological irradiation procedures have been described in detail previously. Before microbeam irradiation, an 8 μm thick polyimide film was floated on the membrane surface and the media was removed to keep the cells hydrated during irradiation and to prevent microbiological contamination due to exposure to room air, which was for less than 20 min depending on the dose and type of radiation. A total of 256 (16 × 16) points within a 15 × 15 mm area in the center of the microbeam dishes were irradiated using a microbeam spot of 5 μm in diameter (Fig. 1B). Within each spot, when one traversal of carbon ion, neon ion or argon ion (equivalent to 0.05, 0.2 and 0.6 Gy, respectively) was delivered (Table 1), the fraction of cells in targeted by a primary ion in the exposed populations was estimated to be 0.036–0.144%. Therefore, under these conditions, the vast majority of the cells could be considered as nondirectly targeted cells (i.e., presumably bystanders) and the contribution of effects induced in cells hit by a primary particle to the overall response of the exposed cultures should be negligible.

Immediately after irradiation, fresh growth medium was added to the microbeam dishes, and the cultures were incubated at 37°C in 95% air/5% $CO_2$ humidified atmosphere. The absorbed dose (Gy) by NB1RGB cells due to a traversal by any of a number of ions through a single target cell (Table 1) was calculated as the fluence (number of ion particles/$cm^2$) converted to dose by using the following formula (22):

$$\mathrm{Dose(Gy)}=\mathrm{fluence(ions/cm^2)} \times \mathrm{LET(keV/\mu\,m)} \times 1.602 \times 10^{-9}$$

In all of the experiments, sham-irradiated cells were subjected to exactly the same manipulations as the irradiated cells. The exposure time varied from 7 to 20 min depending on the radiation dose.

## Micronucleus Formation

The fraction of micronucleated cells in the exposed cultures was assessed using the cytokinesis block technique (31). Briefly, at 4 h after irradiation, irradiated cell populations and their respective controls were subcultured and ~$3 \times 10^4$ cells were seeded in chamber flaskettes (Nalgene Nunc, Rochester, NY) and allowed to grow in the presence of 2 μg/ml cyctochalasin B (Sigma, St. Louis, MO). After 72 h incubation at 37°C, the cells were rinsed in phosphate buffered saline (PBS), fixed in ethanol, stained with Hoechst 33342 solution (1 μg/ml in PBS) (Molecular Probes, Eugene, OR) and viewed under a fluorescence microscope (Zeiss Axioplan2 imagine, Germany). At least 500–1,000 cells were examined for each data point, and only micronuclei in binucleated cells were considered for the analysis. At the concentration used, cytochalasin B was not toxic to NB1RGB cells (Figs. 2 and 3).

## Inhibition of Gap Junction Communication

We dissolved 18-α-glycyrrhetinic acid (AGA) (Sigma, St. Louis, MO), a reversible inhibitor of gap junction communication, in dimethyl sulfoxide (DMSO) and added the mixture to cell cultures at a nontoxic concentration (50 μ*M*), 30 min prior to irradiation. Immediately after irradiation, fresh growth medium containing AGA was added to the dishes and the cultures were then incubated in a 95% air/5% $CO_2$ humidified incubator at 37°C until they were trypsinized 4 h after irradiation and assayed for MN formation. Control cell cultures were incubated in growth medium containing the dissolving vehicle.

## Transfer of Growth Medium

The protocol described by Mothersill and Seymour was used (12, 13). Confluent NB1RGB fibroblasts were irradiated with the equivalent dose of 0.4 Gy from 5.35-keV monochromatic X-ray microbeam at the KEK. The irradiation procedure has been described in detail previously. After irradiation, irradiated cells were returned to the incubator at 37°C. Within 4 h postirradiation, the culture medium was collected and passed through a 0.2-μm filter with low-protein binding characteristics (Millipore, Ireland) to remove floating cells and cellular debris. This cell-free filtrate was considered to be conditioned medium and was transferred to nonirradiated cell cultures. The cultures were incubated for 4 h and MN formation was examined as described above. Control cells received either fresh medium or

conditioned medium from a nonirradiated donor dish. There was no significant difference between these control groups (data not shown).

### Monte Carlo Track Structure Simulations

The complex succession of events that follows the irradiation of matter is stochastic in nature. Therefore, the software Relativistic Ion Tracks (RITRACKS) is a Monte Carlo simulation code used to simulate radiation tracks for heavy ions and electrons in matter (32, 33). In principle any ion track can be simulated if the energy is within the range of which the cross sections for interactions of primary particles and secondary electrons with target molecules are known. The RITRACKS program is used to simulate the so-called physical and physicochemical stages of the radiolysis of water (34). The ion is followed on an event-by-event basis, calculating all ionization and excitation events produced and recording the position of the generated radiolystic species, and the energy and the direction of the secondary electrons. This code uses recently revisited ionization and excitation cross sections, which takes the effective charge of the ion and relativistic corrections into account (33). Similarly, the produced electrons are followed by the electron transport part of the code, which also simulates the ionization, electronic excitation, elastic collisions and dissociative attachment events. RITRACKS has been validated by the calculations of dosimetric relevant quantities such as the stopping power and electron penetration range. For example, the radial dose distributions of ions calculated from RITRACKS are able to reproduce successfully experimental data and calculation from amorphous tracks (33). The dose deposited by the radiation can be calculated in microvolumes and nanovolumes (35, 36). In this study, to reproduce the effect of X rays, we used in the simulation protons with average LET value of ~6 keV/μm.

### Statistical Analysis

The data presented are representative of at least 3 separate experiments, and we used Poisson statistics to calculate the standard errors associated with the percentage of micronucleated cells in the total number of binucleated cells. Comparisons between treatment groups and respective controls were performed using Pearson's $\chi^2$ test. A $P$ value of ≤0.05 between groups was considered significant.

## RESULTS

The objective of this study was to investigate whether GJIC mediates the induction of MN formation (a reflection of DNA double-strand breaks) in bystander cells after exposure of other cells in the culture to low-LET radiation or high-LET radiation using X-ray or heavy-ion microbeams, respectively. To this end, we exposed to radiation confluent, density-inhibited human skin fibroblasts that functionally communicate with one another through gap junctions. The cultures were exposed to graded doses from monochromatic 5.35 keV X rays (LET ~6 keV/μm), 18.3 MeV/u carbon ions (LET ~103 keV/μm), 13 MeV/u neon ions (LET ~380 keV/μm) or 11.5 MeV/u argon ions (LET ~1,260 keV/μm), by which only 0.036–0.144% of cells in the populations were directly traversed by an IR track. Four hours of incubation at 37°C allowed communication between irradiated and nonirradiated cells, which likely included junctional and nonjunctional modes of communication. The cells were

then subcultured and assayed for MN formation. The results showed that micronucleus formation was dose-dependent with any of the radiation sources and was greater than expected based on the fraction of cells irradiated (Fig. 2). As can be seen in Fig. 2, high-LET heavy-ion microbeams were more effective than low-LET X-ray microbeam in the induction of DNA damage in bystander cells. Interestingly, the dose-dependent increase in MN formation induced by low-LET X rays (Fig. 2A) was similar to that induced by high-LET carbon ions at doses between 0.1 and 0.4 Gy, implying similar magnitude of bystander effects (Fig. 2B). However, it should be noted that the culture medium was removed from the microbeam dishes during irradiation with heavy-ion microbeams. This is in contrast to the irradiation procedure with low-LET X-ray microbeams. Therefore, the potential contribution of medium-mediated bystander signaling during the irradiation was not adequately accounted for in high-LET-radiation microbeam exposures.

Next, we investigated whether the transfer of medium from X-irradiated culture to nonirradiated cells also caused MN formation in the bystander cells. The data in Fig. 3 show the level of MN formation in bystander cells incubated for 4 h in conditioned medium harvested 4 h post-exposure of targeted cells to 0.4 Gy. Compared with the corresponding sham-irradiated controls, the fraction of bystander cells harboring micronuclei increased by ~60% ($P < 0.05$) when bystander cell populations were cultured with conditioned medium from irradiated cells. Importantly, this suggests that the X-irradiated cells secreted clastogenic molecules into the culture medium, and this medium was capable of inducing a DNA damage response in nonirradiated bystander cells (12–14, 37). Taken together our results show that secreted factors play a critical role in inducing stressful bystander effect during confluent holding. Consequently, it is necessary to consider the potential influence of medium transfers in cell cultures exposed to high-LET-radiation microbeams, as this may compound the effect observed in Fig. 2 where the role of secreted factors may have been missed due to replacement of the medium with fresh medium immediately after irradiation.

Previous reports have demonstrated that GJIC mediates the propagation of stressful effects in bystander cells exposed to high-LET radiation by which only 1–2% of cell in the population is traversed by an IR track (21, 23). Here, we further pursue these earlier findings and investigate the role of GJIC between irradiated cells and bystander cells in modulating bystander MN formation after exposure to low-LET radiation or high-LET radiation. We hypothesized that GJIC contributes to the propagation of stressful effects between irradiated cells and bystander cells during confluent holding in manner dependent on radiation quality. To test this hypothesis, we exposed confluent cells to low- or high-LET-radiation microbeams, in the presence of the gap junction inhibitor AGA. The cells were then held in confluence at 37°C for 4 h in the incubator prior to subculturing. The data in Fig. 2B and D show a significant ($P < 0.05$ and $P < 0.0005$) decrease in the MN formation in bystander cells incubated with AGA following exposure to high-LET radiation. Interestingly, significant attenuation of MN formation occurred in bystander cells at all doses of high-LET neon ions and argon ions delivered to targeted cells, but not when the targeted cells were exposed to high-LET carbon ions (Fig. 2B–D). In contrast, incubation of the cells with AGA did not significantly affect the induction of DNA damage in bystander cells during confluent holding after low-LET X irradiation (Fig. 2A). Taken together, these data indicate that the

stressful effect in bystander cells exposed to high-LET radiation but not low-LET radiation is amplified mainly by GJIC.

It is well established that energy deposition by certain high-LET particulate radiation can be widespread and may extend a significant distance from the core of the primary IR track, which arise mainly by secondary radiation, particularly δ rays (38, 39). The ranges of δ rays produced after high-LET radiation such as high energy and high atomic number (HZE) particles can extend up to several cell diameters (40, 41). The cells traversed by δ rays may therefore also experience biological change. Thus, we simulated the structure of the tracks resulting from exposure of biological matter to the radiation used in this study (X rays or energetic carbon, neon or argon ions) by using the RITRACKS software taking account of the low-LET δ rays. As shown in Fig. 4 and Table 2, a primary track of high-LET radiation is densely ionizing and generates extensive δ rays with a significant range. The data in Fig. 5 represent the radial dose distributions for high-LET radiation (carbon, neon and argon). As expected, a decrease in absorbed dose correlate with increase in radial distance from the core of the track of the primary ion.

## DISCUSSION

We tested the hypothesis that the propagation of stressful effects from irradiated normal mammalian cells to bystander cells greatly depend on intercellular communication and occurs in a manner dependent on radiation quality and dose. Confluent normal human fibroblasts were exposed to X-ray or heavy-ion microbeams using the 256 (16 × 16) cross-strip method (Fig. 1), in which the nucleus and/or cytoplasm of cells could be targeted and irradiated. Typically, the area of microbeam dish is $1.017 \times 10^9$ μm$^2$, containing an average of $7.2 \times 10^5$ cells. Therefore, the area of a cell is estimated to be ~$1.413 \times 10^3$ μm$^2$. Based on these facts, the percentage of irradiated cells for 256 cross-strip method is ~0.036%. However, if the single traversal hit the edge of cytoplasm of a cell, the maximum number of cells in the exposure area would be 4 cells. Thus, the percentage of the irradiated cells in this case is ~0.144%. As a result, the percentage of irradiated cells among the whole cell populations is 0.036–0.144%. In addition, the beam interval (1 mm) is much larger than the size of cells (Fig. 1B). This indicates that a single cell does not receive any multiple hits in our method. Moreover, in our experimental condition, about 720,000 cells were plated and irradiated. Of these cells, about 30,000 cells were replated for the MN assay whereby at least 500–1,000 binucleated cells were scored. This means that the scored cells represented ~0.07–0.14% of the initially exposed cell population. Our results showed that the percentage of MN formation was ~1.5–9% in the absence of the GJIC inhibitor AGA and ~1–4.5% in the presence of AGA compared with ~1% of MN in control cells (Fig. 2). If MN formation can occur only in directly irradiated cells, then the percentage of MN formation could never go above 3.85%, assuming no bystander effects. However, our data gave results beyond our expectation. This is clear evidence that the induction of DNA damage in bystander cells occurs in cell populations in which 0.036–0.144% of total cells are targeted by primary irradiation from low- or high-LET radiation microbeams.

Here we show that the magnitude of bystander responses was dependent on the LET and dose of radiation (Fig. 2). These results fit well with the recent studies of refs. (42, 43),

which demonstrated LET dependence of stressful bystander effects evaluated by the endpoint of MN formation. Notably, the progeny of bystander cells that were co-cultured with cells irradiated with high-LET iron, but not low-LET protons, and allowed to grow for 20 generations showed a decrease in cloning efficiency, an increase in MN formation and higher levels of oxidative stress (44), and were more prone to neoplastic transformation than respective controls (45). Therefore, strong evidence indicates short- and long-term effects in bystander cells depend on radiation quality (1–17, 19–25, 42–47).

The results described here contrast with the published data of Sowa *et al*. (18) showing that there was no statistically significant evidence of a medium transfer bystander effect after exposure to low-LET γ rays but there was a significant medium transfer bystander effect after exposure to high-LET α particles. This apparent variability in the effect may arise from a wide variety of factors, including cell phenotype, radiation quality, ion species, dose range, dose rate, experimental protocols, timing and endpoints (11, 20, 23). Whereas certain factor(s) in the growth medium may inhibit the production of the bystander response (20), the density of cell cultures may enhance a bystander response mediated by secreted factors being released into the culture medium after irradiation (3, 12). In our studies, a medium transfer bystander effect was observed after exposure to low-LET X rays (Fig. 3) as highlighted by the induction of MN formation. These results show that a moderate dose of low-LET X rays (LET ~6 keV/um) may producing a bystander stress response mediated through indirect mode of intercellular communication. In this context, bystander effects induced by high-LET microbeams may be greater than we had previously thought which, may translate in greater health risks (47, 48).

The mechanism(s) of bystander effects are likely to be complex and involve multiple pathways (4, 20, 49, 50). There appear to be at least two different mechanisms by which bystander effects are propagated. In confluent cultures, GJIC may be a critical mediator of the bystander response in cell populations exposed to microbeams (19–25). The stressful effects in cells exposed to high-LET radiation are amplified mainly by GJIC (Fig. 2) perhaps through the spread of toxic molecules from irradiated cells (24, 25). In contrast, under low-LET irradiation conditions (Figs. 2 and 3), secretion of a cytotoxic factor (e.g., long-lived oxidizing molecules, cytokines) may be involved (4, 17, 20, 44–47). In particular, pathways that perturb oxidative metabolism are likely to be important in both mechanisms (4, 20, 39, 49, 50). The propagation of toxic molecules from irradiated cells to bystander cells may overwhelm DNA-repair activities and perturb oxidative metabolism, which would increase the level of spontaneous DNA damage (37). In contrast, inhibition of GJIC by AGA prevents the propagation of damaging signals to bystander cells, thus allowing their protective mechanisms to deal solely with damage due to spontaneous oxidative stress (44). The differential effects observed in cells exposed to low- or high-LET microbeam irradiation suggest that molecules with different effects or different amounts of the same molecules may be propagated under these irradiation conditions (Fig. 2). Additional investigation is required to elucidate the nature of bystander signaling molecules transmitted by irradiation by gap junctions that promote the biological effects in bystander cells, and the findings of such investigation may help to explain this hypothesis.

The Monte Carlo simulation studies in Fig. 4 reflect the complexity of high-LET microbeam irradiation (Fig. 4 and Table 2), which results in significant dose deposited due to low-LET δ rays with range from ~3.5–15 μm (LET~0.8–1.1 keV/μm). These δ rays can potentially irradiate and produce biochemical changes in nearby NB1RGB cells (diameter of ~13.5 μm) (41). Therefore, the cells exposed to low-LET δ rays may experience up-regulation of protective rather than damaging effects, and could attenuate the damaging effects propagated from cells traversed by primary energetic neon or argon particles (41). Conversely, truly bystander cells in the exposed population may also transmit rescuing signals to the irradiated cells (51, 52). Therefore, the overall response of the cell population depends not only on the pattern of energy deposition (53), but also on the extensive network of intercellular communication between targeted and nontargeted cells.

In conclusion, by using microbeam irradiation, this study extends the established role of GJIC in the propagation of stressful effects between irradiated and bystander cells, and shows the importance of radiation quality, radiation dose and track structure on these effects. Based on the observations in this study, it is reasonable to suggest that GJIC and/or soluble factors-mediated processes contribute to the bystander response in human skin fibroblasts exposed to low- or high-LET radiation during confluent holding. The results clearly show the usefulness of microbeam irradiation in understanding the modes of intercellular communication that mediate low- and high-LET-induced bystander effects. Understanding the mechanisms underlying these effects is relevant to cancer therapy with energetic heavy ions and to radiation protection, especially during prolonged space travel.

## Acknowledgments

The authors acknowledge the excellent help from all the support personnel at TIARA, KEK and NIRS, especially Dr. Cuihua Liu, Ms. Yumiko Kaneko and Ms. Toshie Iizuka. This study was supported in part by JSPS KAKENHI Grant Number 23–01513, 18310042, 24620014 and the Quantum Beam Technology Program from the Japan Science and Technology Agency.

## References

1. Nagasawa N, Little JB. Induction of sister chromatid exchanges by extremely low dose of alpha-particles. Cancer Res. 1992; 52:6394–6396. [PubMed: 1423287]
2. Little JB. Genomic instability and bystander effects: a historical perspective. Oncogene. 2003; 22:6978–6987. [PubMed: 14557801]
3. Mothersill C, Seymour CB. Radiation-induced bystander effects–implications for cancer. Nat Rev Cancer. 2004; 4:158–164. [PubMed: 14964312]
4. Azzam EI, de Toledo SM, Little JB. Oxidative metabolism, gap junctions and the ionizing radiation-induced bystander effect. Oncogene. 2003; 22:7050–7057. [PubMed: 14557810]
5. Azzam EI, de Toledo SM, Gooding T, Little JB. Intercellular communication is involved in the bystander regulation of gene expression in human cells exposed to very low fluences of alpha particles. Radiat Res. 1998; 150:497–504. [PubMed: 9806590]
6. Zhou H, Suzuki M, Randers-Pehrson G, Vannais D, Chen G, Trosko JE, et al. Radiation risk at low doses may be greater than we thought. Proc Natl Acad Sci USA. 2001; 98:14410–14415. [PubMed: 11734643]
7. Belyakov OV, Malcolmson AM, Folkard M, Prise KM, Michael BD. Direct evidence for a bystander effect of ionizing radiation in primary human fibroblasts. Br J Cancer. 2001; 84:674–679. [PubMed: 11237389]

8. Bishayee A, Rao DV, Howell RW. Evidence for pronounced bystander effects caused by nonuniform distribution of radioactivity using a novel three dimensional tissue culture model. Radiat Res. 1999; 152:88–97. [PubMed: 10428683]
9. Howell RW, Bishayee A. Bystander effects caused by nonuniform distributions of DNA-incorporated 125I. Micron. 2002; 33:127–132. [PubMed: 11567881]
10. Hall E, Hei TK. Genomic instability and bystander effect induced by high LET radiation. Oncogene. 2003; 22:7034–7042. [PubMed: 14557808]
11. Boyd M, Ross SC, Dorrens J, Fullerton NE, Tan KW, Zalutsky MR, et al. Radiation-induced biologic bystander effect elicited in vitro by targeted radiopharmaceuticals labeled with alpha-, beta-, and auger electron-emitting radionuclides. J Nucl Med. 2006; 47:1007–1015. [PubMed: 16741311]
12. Mothersill C, Seymour CB. Medium from irradiated human epithelial cells but not human fibroblasts reduce the clonogenic survival of unirradiated cells. Int J Radiat Biol. 1997; 71:421–427. [PubMed: 9154145]
13. Mothersill C, Seymour CB. Cell-cell contact during gamma irradiation is not required to induce a bystander effect in normal human keratinocytes: Evidence for release during irradiation of a single controlling survival into the medium. Radiat Res. 1998; 149:256–262. [PubMed: 9496888]
14. Suzuki M, Zhou H, Randers-Pehrson G, Hei TK. Effect of medium on chromatin damage in bystander mammalian cells. Radiat Res. 2004; 162:264–269. [PubMed: 15332998]
15. Smilenov LB, Hall EJ, Bonner WM, Sedelnikova OA. A microbeam study of DNA double-strand breaks in bystander primary human fibroblasts. Radiat Prot Dosim. 2006; 122:256–259.
16. Hu B, Wu L, Han W, Zhang L, Chen S, Xu A, et al. The time and spatial effects of bystander response in mammalian cells induced by low dose radiation. Carcinogenesis. 2006; 27:245–251. [PubMed: 16150894]
17. Mothersill C, Stamato TD, Perez ML, Cummins R, Mooney R, Seymour CB. Involvement of energy metabolism in the production of bystander effects by radiation. Br J Cancer. 2000; 82:1740–1746. [PubMed: 10817512]
18. Sowa MB, Goetz W, Baulch JE, Pyles DN, Dziegielewski J, Yovino S, et al. Lack of evidence for low-LET radiation induced bystander response in normal human fibroblasts and colon carcinoma cells. Int J Radiat Biol. 2010; 86:102–113. [PubMed: 20148696]
19. Suzuki M, Tsuruoka C. Heavy charged particles produce a bystander effect via cell-cell junctions. Biol Sci Space. 2004; 18:241–246. [PubMed: 15858391]
20. Hei TK, Zhou H, Lvanov VN, Hong M, Liberman HB, Brenner DJ, et al. Mechanism of radiation-induced bystander effects: a unifying model. J Pharm Pharmacol. 2008; 60:943–950. [PubMed: 18644187]
21. Azzam EI, de Toledo SM, Little JB. Direct evidence for the participation of gap-junction mediated intercellular communication in the transmission of damage signals from alpha-particle irradiated to non-irradiated cells. Proc Natl Acad Sci USA. 2001; 98:473–478. [PubMed: 11149936]
22. Harada K, Nonaka T, Hanada N, Sakarai H, Hasegawa M, Funayama T, et al. Heavy-ion-induced bystander killing of human lung cancer cells: role of gap junctional intercellular communication. Cancer Sci. 2009; 100:684–688. [PubMed: 19469013]
23. Gaillard S, Pusset D, De Toledo SM, Fromm M, Azzam EI. Propagation distance of the alpha-particle-induced bystander effect: the role of nuclear traversal and gap junction communication. Radiat Res. 2009; 171:513–520. [PubMed: 19580486]
24. Shao C, Furusawa Y, Aoki M, Ando K. Role of gap junctonal intercellular communication in radiation-induced bystander effects in human fibroblasts. Radiat Res. 2003; 160:318–323. [PubMed: 12926990]
25. Shao C, Furusawa Y, Matsumoto Y, Pan Y, Xu P, Chen H. Effect of gap junctional intercellular communication on radiation response in neoplastic human cells. Radiat Res. 2007; 167:283–288. [PubMed: 17316077]
26. Harris AL. Emerging issues of connexin channels: biophysics fills the gap. Q Rev Biophys. 2001; 34:325–472. [PubMed: 11838236]

27. Usami N, Maeda M, Eguchi-Kasai K, Maezawa H, Kobayashi K. Radiation-induced γ-H2AX in mammalian cells irradiated with a synchroton x-ray microbeam. Radiat Prot Dosim. 2006; 122:307–309.
28. Maeda M, Usami N, Kobayashi K. Low-dose hypersensitivity in nucleus-irradiated V79 cells studied with synchrotron x-ray microbeam. J Radit Res (Tokyo). 2008; 49:171–180.
29. Terasima T, Tolmach LJ. Changes in X-ray sensitivity of HeLa cells during the division cycle. Nature. 1961; 190:1210–1211. [PubMed: 13775960]
30. Funayama T, Wada S, Yokota Y, Fukamoto K, Sakashita T, Taguchi M, et al. Heavy-ion microbeam system in JAEA for microbeam biology. J Radiat Res (Tokyo). 2008; 49:71–82. [PubMed: 18174669]
31. Fenech M, Morley AA. Measurement of micronuclei in lymphocytes. Mutat Res. 1985; 147:29–36. [PubMed: 3974610]
32. Plante I, Cucinotta F. Cross sections for the interactions of 1 eV–100 MeV electrons in liquid water and application to Monte-Carlo simulation of HZE radiation tracks. New J Phys. 2009; 11:063047.
33. Plante I, Cucinotta F. Ionization and excitation cross sections for the interaction of HZE particles and application to Monte-Carlo simulation of radiation tracks. New J Phys. 2008; 10:125020.
34. Cobut V, Frongillo Y, Patau JP, Goulet T, Fraser M-J, Jay-Gerin J-P. Monte-Carlo simulation of fast electron and proton tracks in liquid water-I. Physical and physicochemical aspects. Radiat Phys Chem. 1998; 51:229–243.
35. Plante I, Cucinotta F. Energy deposition and relative frequency of hits of cylindrical nanovolume in medium irradiated by ions: Monte-Carlo simulation of track structure. Radiat Environ Biophys. 2010; 49:5–13. [PubMed: 19916014]
36. Plante I, Ponomarev AL, Cucinotta FA. 3D visualization of the irradiation dose by a Monte-Carlo simulation of the HZE particle track structure, and the application to the calculation of DSBs in cell nuclei. Radiat Prot Dosim. 2011; 143:156–161.
37. Yang H, Assad N, Held KD. Medium-mediated intercellular communication is involved in bystander responses of X-ray-irradiated normal human fibroblasts. Oncogene. 2005; 24:2096–2103. [PubMed: 15688009]
38. Nikjoo H. Radiation track and DNA damage. Iran J Radiat Res. 2003; 1:3–16.
39. Hill MA. Radiation damage to DNA: The importance of track structure. Radiat Measure. 1999; 31:15–23.
40. Kiefer J, Straaten H. A model of ion track structure based on classical collision dynamics. Phys Med Biol. 1986; 31:1201–1209. [PubMed: 3786407]
41. Gonon G, Groetz J-E, de Toledo SM, Howell RW, Fromm M, Azzam EI. Nontargeted stressful effects in normal human fibroblasts cultures exposed to low fluences of high charge, high-energy (HZE) particles: kinetics of biologic responses and significance of secondary radiations. Radiat Res. 2013; 179:444–457. [PubMed: 23465079]
42. Wakatsuki M, Magpayo N, Kawamura H, Held KD. Differential bystander signaling between radioresistant chondrosarcoma cells and fibroblasts after X ray, proton, iron ion and carbon ion exposures. Int J Radiat Oncol Bio Phys. 2012; 84:103–108.
43. Anzenberg V, Chanairamani S, Coderre JA. LET-dependent bystander effects caused by irradiation of human prostate carcinoma cells with X-rays and alpha particles. Radiat Res. 2008; 170:467–476. [PubMed: 19024654]
44. Buonano M, de Toledo SM, Pain D, Azzam EI. Long-term consequences of radiation-induced bystander effects depend on radiation quality and dose and correlate with oxidative stress. Radiat Res. 2011; 175:405–415. [PubMed: 21319986]
45. Buonano M, de Toledo SM, Azzam EI. Increased frequency of spontaneous neoplastic transformation in progeny of bystander cells from cultures exposed to densely ionizing radiation. Plos One. 2011; 6:e21540. [PubMed: 21738697]
46. Shao C, Furusawa Y, Kobayashi Y, Funayama T, Wada S. Bystander effect induced by counted high-LET particles in confluent human fibroblasts: a mechanistic study. FASEB J. 2003; 82:393–399.
47. Blyth BJ, Sykes PJ. Radiation-induced bystander effects: What are they, and how relevant are they to human radiation exposures? Radiat Res. 2011; 176:139–157. [PubMed: 21631286]

48. Brenner DJ, Little JB, Sachs RK. The bystander effect in radiation oncogenesis II: A quantitative model. Radiat Res. 2001; 155:402–408. [PubMed: 11182790]

49. Hamada N, Matsumoto H, Hara T, Kobayashi Y. Intercellular and intracellular signaling pathways mediating ionizing radiation induced bystander effect. J Radiat Res (Tokyo). 2007; 48:87–95. [PubMed: 17327686]

50. Matsumoto H, Hamada N, Takahashi A, Kobayashi Y, Ohnishi T. Vanguards of paradigm shift in radiation biology: Radiation-induced adaptive and bystander response. J Radiat Res (Tokyo). 2007; 48:97–106. [PubMed: 17327685]

51. Chen S, Zhao Y, Han W, Chiu SK, Zhu L, Wu L, Yu KN. Rescue effects in radiobiology: unirradiated bystander cells assist irradiated cells through intercellular signal feedback. Mutat Res. 2011; 706:59–64. [PubMed: 21073884]

52. Kadhim MA, Moore SR, Goodwin EH. Interrelationships amongst radiation-induced genomic instability, bystander effects, and the adaptive response. Mutat Res. 2004; 568:21–32. [PubMed: 15530536]

53. Deperas-Standylo J, Lee R, Ayriyan A, Nasonova E, Ritter S, Gudowska-Nowak E. Time-course of aberration and their distribution: impact of LET and track structure. Eur Phys J. 2010; 60:93–99.

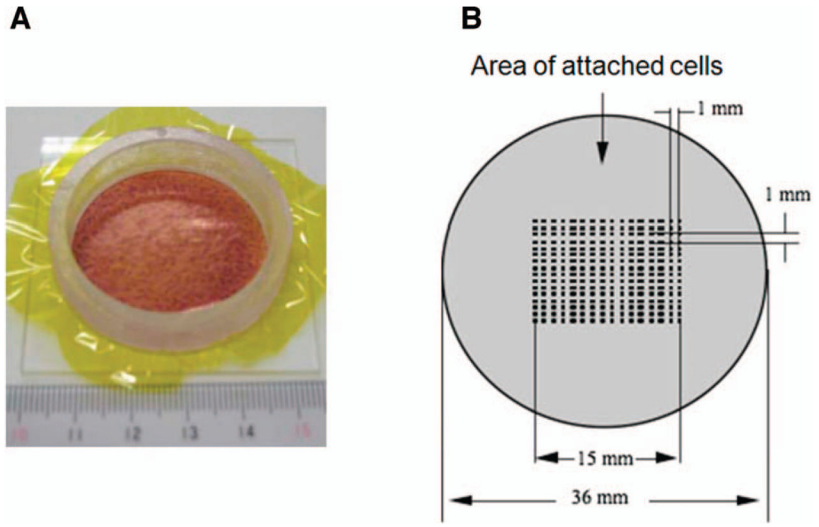


**FIG. 1.**

Microbeam-irradiation procedure of normal human fibroblasts using a 256 (16 × 16) cross-stripe method. A microbeam dish was constructed with an acrylic resin ring of 36 mm diameter and 7.5 μm-thick polyimide films attached to the bottom of the ring. Panel A: Irradiated cells in a confluent state stained with 20% methanol and 0.2% crystal violet. Pane1 B: 16 × 16 points within a 15 × 15 mm areas in the center dish were irradiated using microbeams.

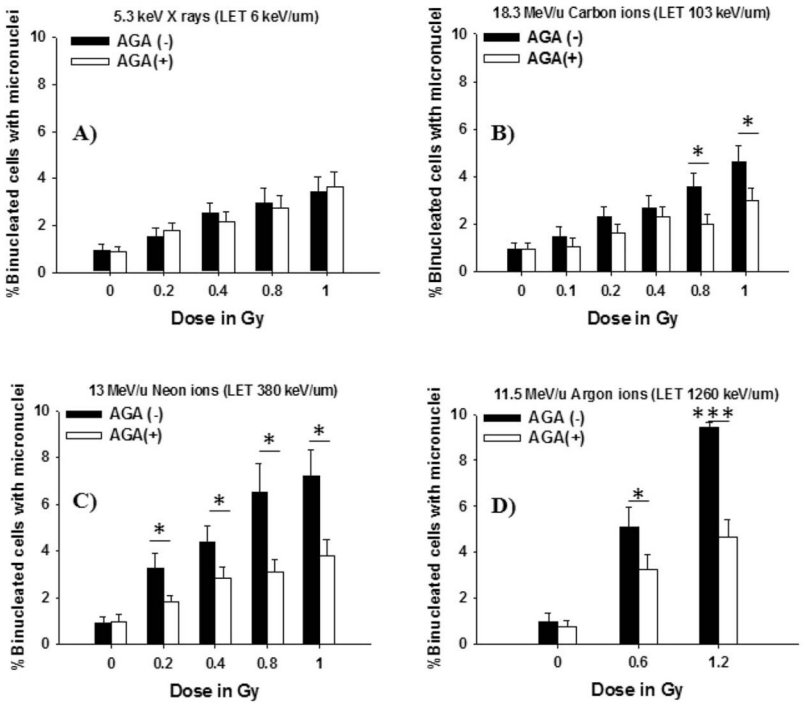


**FIG. 2.**

Role of gap junction communication in the propagation of stressful effects in human cells exposed to low-LET radiation or high-LET radiation. Confluent human skin fibroblasts were exposed to different types of microbeam in the absence (■) or presence (□) of the gap junction inhibitor 18-α-glycyrrhetinic acid (AGA) and holding in the confluent state for 4 h at 37°C then the cells were subcultured and assayed for micronucleus formation: Dose response for frequency of micronuclei formation in bystander NB1RGB cells (panel A: X rays, panel B: carbon ions, panel C: neon ions and panel D: argon ions) (*$P < 0.05$; ***$P < 0.0005$).

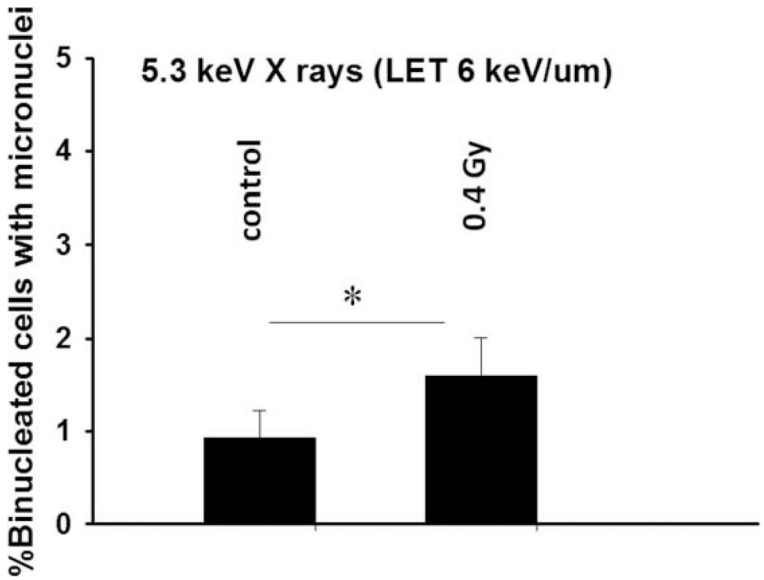


**FIG. 3.**

Effect of medium-mediated cytotoxic factor released from X-irradiated cells to bystander cells: Fraction of micronucleated cells in control and bystander cells (*$P < 0.05$).

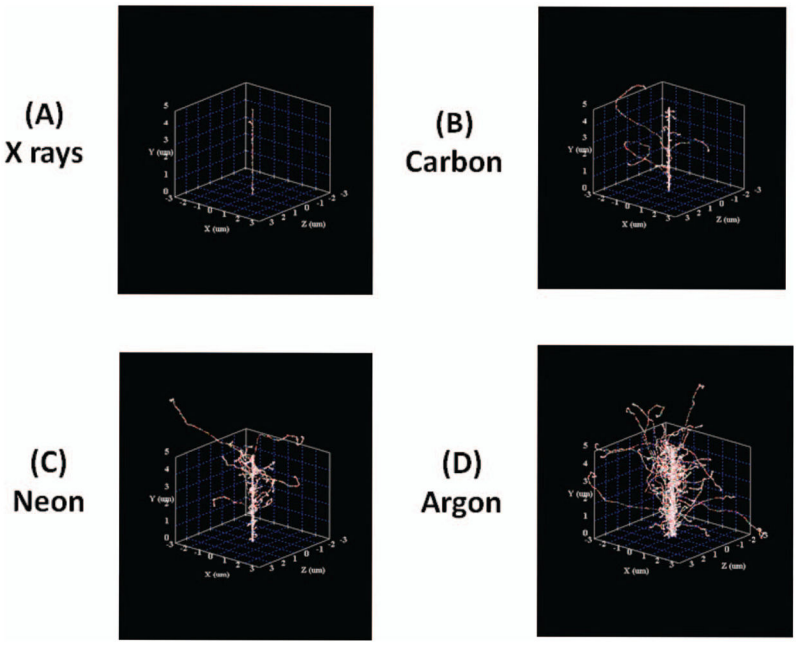


**FIG. 4.**

Monte Carlo track structures simulation. The radiation track structures (panel A: X rays, panel B: carbon ions, panel c: neon ions and panel d: argon ions).

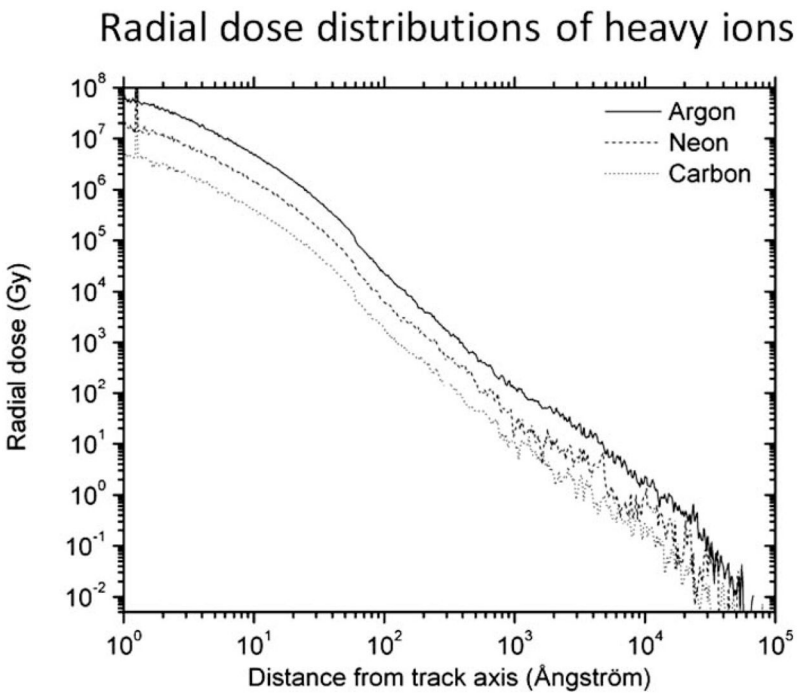


**FIG. 5.**
Calculation of radial dose profiles of high-LET microbeam. Results from track calculations.

## TABLE 1

Physical properties of Microbeams at KEK and TIARA

| Types of microbeams | Energy | LET (keV/μm) | Absorbed dose (Gy) to a target cell |
|---|---|---|---|
| X rays | 5.35 keV | 6 | 0.37 |
| Carbon ions | 18.3 MeV/u | 103 | 0.05* |
| Neon ions | 13 MeV/u | 380 | 0.2* |
| Argon ions | 11.5 MeV/u | 1260 | 0.6* |

*Dose per traversal.

**TABLE 2**

Physical Properties of Secondary Radiation (δ Rays)

| Types of microbeam | $Energy_{max}$ of δ rays | LET (keV/μm) | Average range (μm) |
|---|---|---|---|
| X rays | 5.4 keV | 3.6 | 0.8 |
| Carbon ions | 40 keV | 0.8 | 3.5 |
| Neon ions | 28 keV | 1.0 | 7.5 |
| Argon ions | 25 keV | 1.1 | 15 |